Probing the Intrinisic Structure and Dynamics of Aminoborane Coordination at Late Transition Metal Centers: Mono(σ-BH) Binding in [CpRu(PR$_3$)$_2$(H$_2$BNCy$_2$)]$^+$

Dragoslav Vidovic,* David A. Addy, Tobias Krämer, John McGrady,* and Simon Aldridge*

Inorganic Chemistry Laboratory, Department of Chemistry, University of Oxford, South Parks Road, Oxford OX1 3QR, U.K.

Division of Chemistry and Biological Chemistry, School of Physical and Mathematical Sciences, Nanyang Technological University, 21 Nanyang Link, Singapore 637371

S Supporting Information

ABSTRACT: Aminoboranes, H$_2$BNRR′, represent the monomeric building blocks from which novel polymeric materials can be constructed via metal-mediated processes. The fundamental capabilities of these compounds to interact with metal centers have been probed through the coordination of H$_2$BNCy$_2$ at 16-electron [CpRu(PR$_3$)$_2$]$^+$ fragments. In contrast to the side-on binding of isoelectronic alkene donors, an alternative mono(σ-BH) mode of aminoborane ligation is established for H$_2$BNCy$_2$, with binding energies only ~8 kcal mol^{-1} greater than those for analogous dinitrogen complexes. Variations in ground-state structure and exchange dynamics as a function of the phosphine ancillary ligand set are consistent with chemically significant back-bonding into an orbital of B—H σ^* character.

Aminoboranes, H$_2$BNRR′, are the subject of significant interest not only as the first-formed products in the dehydrogenation of a class of BN-containing hydrogen storage materials but also as the monomeric building blocks from which a number of novel well-defined inorganic polymers can be constructed.[1] Thus, for example, Manners and co-workers have reported the metal-catalyzed polymerization of methylamineborane, H$_3$B·NMeH$_2$, by ruthenium, rhodium, or palladium complexes to give high-molecular-weight poly(aminoboranes), [H$_2$BNMe(H)]$_n$, i.e., BN analogues of poly(propylene).[2] This transformation is thought to occur via two metal-mediated steps, namely (i) dehydrogenation of H$_3$B·NMeH$_2$ and (ii) polymerization of the monomeric H$_2$BNMe(H) so formed.[2] The fundamental mode(s) of interaction of monomeric aminoboranes with catalytically relevant late transition metal systems are therefore of significant interest.[3−7]

Despite their isoelectronic relationship with 1,1-disubstituted alkenes, the coordination chemistry of aminoboranes has only very recently begun to be examined. To date, the only reported examples of such complexes feature chelating H$_2$BNR$_2$ ligands coordinated to [L$_2$M(H)$_2$]$^{n+}$ fragments via two B—H—M bridges (M = Ru, n = 0; M = Rh, Ir, n = 1; L = N-heterocyclic carbene, tertiary phosphine).[5] Such a coordination geometry contrasts with the classical "side-on" binding mode observed for alkene donors within the same framework.[5b,c] However, the utilization of these 14-electron metal systems, while seemingly

essential to synthetic routes which employ in situ amineborane dehydrogenation, presumably distorts the structural landscape in favor of the four-electron-donating bis(σ-BH) coordination mode over the corresponding (two-electron-donating) side-on π-bound motif. Thus, Alcaraz and Sabo-Etienne report an energetic preference of 14.3 kcal mol^{-1} for the "end-on" bis-(σ-BH) coordination geometry of H$_2$BNH$_2$ at [L$_2$Ru(H)$_2$].[5a]

With a view to investigating the intrinsic two-electron donor capabilities of aminoborane ligands, we have therefore set out to examine the coordination of monomeric H$_2$BNCy$_2$ at 16-electron fragments of the type [CpRu(PR$_3$)$_2$]$^+$. While such metal systems are known to be capable of the side-on binding of alkenes,[8] an alternative mono(σ-BH) mode of aminoborane ligation is established for H$_2$BNCy$_2$. Crystallographic studies in the solid state, together with DFT calculations and spectroscopic studies in solution, allow for the elucidation of ground-state binding motifs/energetics and the dynamic exchange pathways as a function of the ancillary phosphine co-ligands.

The syntheses of aminoborane complexes [CpRu(PR$_3$)$_2$-(H$_2$BNCy$_2$)]$^+$[BAr$^f_4$]$^-$ [(PR$_3$)$_2$ = (PPh$_3$)$_2$ (**5**); Cy$_2$PCH$_2$CH$_2$-PCy$_2$, dcype (**6**)] are readily accomplished according to the chemistry outlined in Scheme 1. In each case, cleaner syntheses are effected through the intermediacy of the dinitrogen complexes [{CpRu(PPh$_3$)$_2$}$_2$(μ-N$_2$)]$^{2+}$[BAr$^f_4$]$^-$$_2$ (**3**)[9] and [CpRu-(dcype)(N$_2$)]$^+$[BAr$^f_4$]$^-$ (**4**) (see Supporting Information); in situ reactivity of **1** (or **2**) with Na[BAr$^f_4$]/H$_2$BNCy$_2$ under an argon atmosphere invariably generates a mixture of Ru/P-containing products. In the case of **4**, subsequent reaction with H$_2$BNCy$_2$ generates **6** in nearly quantitative yield (as judged by multinuclear NMR), with the isolated yield of ca. 30% reflecting losses inherent in the isolation of this very reactive species.[10]

5 and **6** have been characterized by ^{1}H, ^{11}B, ^{13}C, ^{19}F, and ^{31}P NMR spectroscopy, elemental microanalysis, and single-crystal X-ray diffraction. Although the ^{11}B NMR spectrum of each compound features a broad resonance (at δ_B 35 ppm) which is not shifted significantly from the free aminoborane (δ_B 35.4 ppm),[11] the corresponding ^{1}H NMR spectra at 20 °C are more informative, featuring distinct resonances associated with the RuHB and BH hydrogens (at δ_H −11.97 and 6.39 ppm for **5**; −14.56 and 5.80 ppm for **6**, respectively). The ^{31}P NMR spectrum of both compounds at 20 °C displays a single resonance,

Scheme 1. Syntheses of κ^1-Aminoborane Complexes 5 and 6 from the Corresponding Dinitrogen Systems[a]
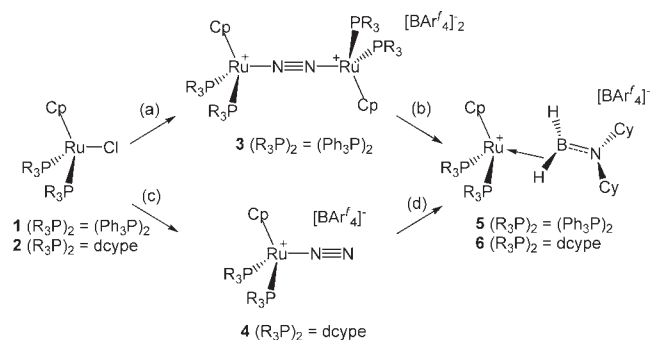

[a] Key reagents/conditions: (a) Na[BAr$^f_4$] (1.0 equiv), fluorobenzene, N_2 atmosphere, 10 min at 20 °C, as per ref 8; (b) H$_2$BNCy$_2$ (1.0 equiv), fluorobenzene, 5 min at 20 °C, 32% isolated yield; (c) Na[BAr$^f_4$] (1.0 equiv), fluorobenzene, N_2 atmosphere, 10 min at 20 °C, quantitative by NMR, ca. 10% isolated yield; (d) H$_2$BNCy$_2$ (1.0 equiv), fluorobenzene, 5 min at 20 °C, 24% isolated yield.
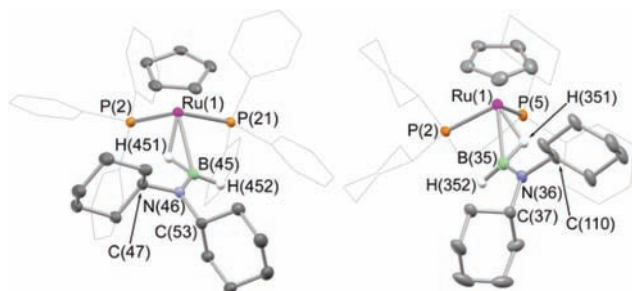
Figure 1. Structures of the cationic components of **5** and **6**. Anions and hydrogen atoms (except boron-bound hydrogens) are omitted, and phosphine substituents are shown in wireframe format for clarity. Thermal ellipsoids are set at the 30% probability level. Key bond lengths (Å) and angles (°): for **5**, Ru(1)−P(2) 2.354(1), Ru(1)−P-(21) 2.358(1), Ru(1)···B(45) 2.430(4), Ru(1)−H(451) 1.665(4), B(45)−N(46) 1.376(4), B(45)−H(451) 1.207(4), B(45)−H(452) 1.114(4), Ru(1)···B(45)−N(46) 130.2(3); for **6**, Ru(1)−P(2) 2.338(1), Ru(1)−P(5) 2.319(1), Ru(1)···B(35) 2.332(6), Ru-(1)−H(351) 1.669(1), B(35)−N(36) 1.382(7), B(35)−H(351) 1.244(6), B(35)−H(352) 1.150(5), Ru(1)···B(35)−N(36) 133.1(4). The boron-bound hydrogen atoms were located in the crystallographic Fourier difference maps.

consistent with averaging of the two phosphorus environments via rapid rotation of the aminoborane ligand about the Ru−(BH centroid) axis (*vide infra*).

While the formulations of both **5** and **6** were suggested by spectroscopic data and the bulk composition confirmed by microanalysis, unequivocal characterization was additionally reliant on crystallographic studies (Figure 1).[12] The structures of the cationic components of these compounds feature in common (i) a three-legged piano stool geometry at ruthenium, with the non-Cp coordination environment being defined by the two phosphorus centers and the B−H centroid [∠(BH centroid)−Ru−P = 90.3, 96.3° and 90.9, 92.0° for **5** and **6**, respectively], and (ii) a mono-(σ-BH) aminoborane ligand characterized by a bent Ru···B−N framework [∠Ru···B−N = 130.2(3)° for **5**, 133.1(4)° for **6**], which contrasts with the analogous (essentially linear) fragment
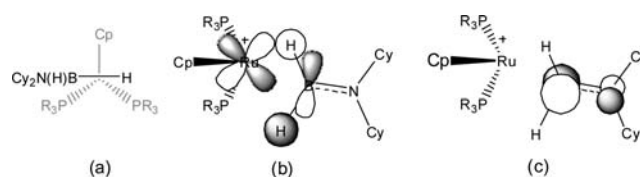
Figure 2. (a) Simplified diagram showing the alignment of the metal and borane fragments in **6**. (b) Alignment of the [CpRu(PR$_3$)$_2$]$^+$ HOMO and borane BH σ* MO. (c) Alignment of the BN π* MO.

found for κ^2-bound H$_2$BNCy$_2$ ligands (e.g., 178.4(3)° for [(IMes)$_2$Rh(H)$_2$(H$_2$BNCy$_2$)]$^+$).[5b,c,13]

Spectroscopically, the presence of a single Ru−H−B bridging interaction is revealed by distinct RuHB and BH signals in the ^{1}H NMR spectra of **5** and **6** at 20 °C and is further signaled by disparate Ru−H and B−H contacts in the solid state (e.g., for **6**, d[Ru(1)−H(351)] = 1.669(1), d[Ru(1)···H(352)] = 2.887 Å; d[B(35)−H(351)] = 1.244(6), d[B(35)−H(352)] = 1.150(5) Å). Moreover, the presence of only one bridging hydrogen atom is consistent with Ru···B distances [2.430(4) and 2.332(6) Å for **5** and **6**, respectively] which are significantly longer than that found in (Cy$_3$P)$_2$Ru(H)$_2$(κ^2-H$_2$BN^{i}Pr$_2$) [1.980(3) Å].[5d] The finding that the Ru···B contacts for **5** and **6** are *shorter* than that in [CpRu(PMe$_3$)$_2$(κ^1-H$_3$B·NMe$_3$)]$^+$ [2.648(3) Å] presumably reflects the presence of a three (rather than four)-coordinate boron center and the possibility for back-bonding from ruthenium.[14,15]

Three additional observations are consistent with the possibility for back-bonding from the highest occupied molecular orbital (HOMO) of the [CpRu(PR$_3$)$_2$]$^+$ fragment into a B−H σ* orbital of the coordinated borane in **5** and **6**. First, the alignment of the coordinated B−H bond with respect to the [CpRu(PR$_3$)$_2$]$^+$ fragment [as manifested, for example, by a (Cp centroid)−Ru−(BH centroid)−B torsion angle of 84.3° for **6**] maximizes the potential for overlap between the respective orbitals (Figure 2a,b).[16] Second, the differences in both the Ru···B [2.430(4), 2.332(6) Å] and B−H(Ru) distances [1.207(4), 1.244(6) Å] between **5** and **6** are consistent with greater back-bonding from the more electron-rich [CpRu(dcype)]$^+$ fragment (cf. [CpRu(PPh$_3$)$_2$]$^+$), albeit with some caution attached to the interpretation of the less well defined B−H distances. Finally, the chemical shift of the RuHB bridging hydrogen is also markedly more hydridic in the case of **6** (δ_H −14.56, cf. −11.97 for **5**). By contrast, the BN distances for the two compounds are statistically identical [1.376(4) and 1.382(7) Å], suggesting little population of the BN π* orbital. Such an observation conflicts with that made for (Cy$_3$P)$_2$Ru(H)$_2$-(H$_2$BN^{i}Pr$_2$) but is not entirely unexpected for the current [CpRu(PR$_3$)$_2$]$^+$ systems, given that the BN π* orbital in **6**, for example, lies effectively orthogonal to the metal-based HOMO (Figure 2c).[16]

Differences in the binding affinity of H$_2$BNCy$_2$ for the ruthenium center in **5** and **6** presumably also influence the fluxional behavior of these systems, as determined by variable-temperature NMR experiments. Thus, **6** is characterized by two fluxional processes relating to the dynamic behavior of the coordinated borane. At very low temperatures (T = −80 °C) in CD$_2$Cl$_2$ solution, the ^{31}P{^{1}H} NMR spectrum of **6** shows two resonances (at δ_P 79.2 and 83.1 ppm; $^2J_{PP}$ = 23 Hz) consistent with the structure of the cation determined crystallographically and with slow rotation about the Ru−(BH centroid) vector on

Scheme 2. Fluxional Processes Involving the B—H Bonds in 5 and 6
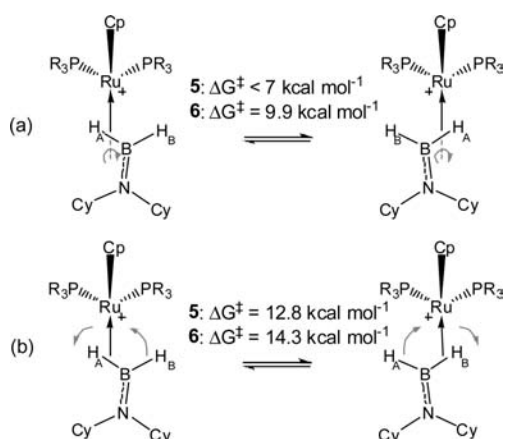
the NMR time scale (Scheme 2a). Coalescence of these resonances occurs at $T = -50\ ^\circ$C, and the barrier to rotation ($\Delta G^\ddagger = 9.9$ kcal mol^{-1}) so determined is marginally greater than the value of 7.4 kcal mol^{-1} reported by Schlecht and Hartwig for a comparable process in CpMn(CO)$_2$(HBcat).[17] By contrast, the analogous fluxional process for **5** cannot be frozen out at temperatures in excess of $-90\ ^\circ$C, suggesting that the corresponding barrier to rotation in this case is less than ca. 7 kcal mol^{-1}. A second fluxional process can be identified for both complexes ($T_c = 7\ ^\circ$C, $\Delta G^\ddagger = 12.8$ kcal mol^{-1} for **5**; $T_c = 28\ ^\circ$C, $\Delta G^\ddagger = 14.3$ kcal mol^{-1} for **6**) which results in coalescence of the RuHB and BH signals and of the two distinct sets of cyclohexyl methine protons. As such, these spectral changes are assigned to a process involving exchange of the bound and unbound BH hydrogens (Scheme 2b), with the markedly higher barrier associated with this process for **6** (vs **5**) being consistent with the tighter binding of the borane implied crystallographically.

In order to quantify/contextualize the strength of the metal–ligand interaction associated with this simple mono(σ-BH) mode of coordination of H$_2$BNCy$_2$, a series of quantum chemical calculations has been carried out on **5**, **6**, and related [CpRu-(PR$_3$)$_2$]$^+$-containing systems (see Supporting Information). Consistent with the structural data determined in the solid state, significantly stronger binding of the aminoborane is found for **6** ($\Delta G = -26.0$ for ligand association, cf. -15.2 kcal mol^{-1} for **5**). Moreover, these free energies can be put into context by the corresponding values of -46.5, -19.2, and -17.2 kcal mol^{-1} calculated for the binding of CO, η^2-C$_2$H$_4$, and N$_2$ to the same cationic [CpRu(dcype)]$^+$ fragment. Experimentally, such data are consistent with the displacement of N$_2$ by H$_2$BNCy$_2$ in the synthesis of **6**, and with the (synthetically verified) reaction of **6** with CO to generate [CpRu(dcype)(CO)]$^+$ and free aminoborane (see Supporting Information). Calculations have also been carried out on **6** to shed light on the likely mechanism for the exchange process shown in Scheme 2b; a transition state can be identified (at a free energy of $+17.5$ kcal mol^{-1} with respect to **6**) featuring a more symmetrically bound aminoborane ligand (d[Ru–H] = 2.261, 2.334 Å; d[B–H] = 1.200, 1.202 Å) and a markedly elongated Ru$\cdots$B separation (2.570 Å), consistent with a concerted nondissociative exchange process in this case.

In summary, we report the first complexes containing an aminoborane ligand coordinated to a 16-electron metal center,

thereby defining the intrinsic two-electron donor capabilities of this topical ligand family. Geometric parameters for the monodentate BH-bound ground-state structures and details of dynamic fluxional processes have been probed as functions of the ancillary phosphine co-ligands. Ru(II) systems have been shown to be among the most active catalysts for the dehydrocoupling/polymerization of methylamineborane;[2] the current study sheds light on coordination geometries and migratory pathways potentially accessible for the aminoborane monomer in catalytic systems. Further details of the reactivity of these novel systems will be reported in due course.

■ **ASSOCIATED CONTENT**

ⓢ Supporting Information. Synthetic and characterization details for **4** and **5**; details of all DFT-calculated structures; crystallographic data for **3**–**6** (CIF). This material is available free of charge via the Internet at http://pubs.acs.org.

■ **AUTHOR INFORMATION**

Corresponding Author
Simon.Aldridge@chem.ox.ac.uk

■ **ACKNOWLEDGMENT**

■ **REFERENCES**

(1) For recent reviews of relevant BN-containing materials, see: (a) Clark, T. J.; Lee, K.; Manners, I. *Chem. Eur. J.* **2006**, *12*, 8634–8648. (b) Marder, T. B. *Angew. Chem., Int. Ed.* **2007**, *46*, 8116–8118. (c) Stephens, F. H.; Pons, V.; Baker, R. T. *Dalton Trans.* **2007**, 2613–2626. (d) Hamilton, C. W.; Baker, R. T.; Staubitz, A.; Manners, I. *Chem. Soc. Rev.* **2009**, *38*, 279–293. (e) Staubitz, A.; Robertson, A. P. M.; Sloan, M. E.; Manners, I. *Chem. Rev.* **2010**, *110*, 4023–4078. (f) Staubitz, A.; Robertson, A. P. M.; Manners, I. *Chem. Rev.* **2010**, *110*, 4079–4124. (g) Alcaraz, G.; Sabo-Etienne, S. *Angew. Chem., Int. Ed.* **2010**, *49*, 7170–7179.

(2) (a) Staubitz, A.; Soto, A. P.; Manner, I. *Angew. Chem., Int. Ed.* **2008**, *47*, 6212–6214. (b) Staubitz, A.; Sloan, M. E.; Robertson, A. P. M.; Friedrich, A.; Schneider, S.; Gates, P. J.; auf der Günne, J. M.; Manners, I. *J. Am. Chem. Soc.* **2010**, *132*, 13332–13345.

(3) For an early spectroscopic report examining aminoborane interactions with transition metals, see: Schmid, G. *Chem. Ber.* **1970**, *103*, 528–533.

(4) Pons, V.; Baker, R. T.; Szymczak, N. K.; Heldebrant, D. J.; Lineham, J. C.; Matus, M. H.; Grant, D. J.; Dixon, D. A. *Chem. Commun.* **2008**, 6597–6599.

(5) (a) Alcaraz, G.; Vendier, L.; Clot, E.; Sabo-Etienne, S. *Angew. Chem., Int. Ed.* **2010**, *49*, 918–920. (b) Tang, C. Y.; Thompson, A. L.; Aldridge, S. *Angew. Chem., Int. Ed.* **2010**, *49*, 921–925. (c) Tang, C. Y.; Thompson, A. L.; Aldridge, S. *J. Am. Chem. Soc.* **2010**, *132*, 10578–10591. (d) Alcaraz, G.; Chaplin, A. B.; Stevens, C. J.; Clot, E.; Vendier, L.; Weller, A. S.; Sabo-Etienne, S. *Organometallics* **2010**, *29*, 5591–5595. (e) Stevens, C. J.; Dallanegra, R.; Chaplin, A. B.; Weller, A. S.; Macgregor, S. A.; Ward, B.; McKay, D.; Alcaraz, G.; Sabo-Etienne, S. *Chem. Eur. J.* **2011**, *17*, 3011–3020.

(6) For studies of catalytic systems for the dehydrogenation of B/N-based materials based on group 9 metals, see, for example: (a) Jaska, C. A.; Temple, K.; Lough, A. J.; Manners, I. *J. Am. Chem. Soc.* **2003**, *125*, 9424–9434. (b) Jaska, C. A.; Manners, I. *J. Am. Chem. Soc.* **2004**, *126*, 9776–9785. (c) Jaska, C. A.; Clark, T. J.; Clendenning, S. B.; Grozea, D.; Turak, A.; Lu, Z.-H.; Manners, I. *J. Am. Chem. Soc.* **2005**,

127, 5116–5124. (d) Denney, M. C.; Pons, V.; Hebden, T. J.; Heinekey, D. M.; Goldberg, K. I. *J. Am. Chem. Soc.* **2006**, *128*, 12048–12049. (e) Fulton, J. L.; Linehan, J. C.; Autrey, T.; Balasubramanian, M.; Chen, Y.; Szymczak, N. K. *J. Am. Chem. Soc.* **2007**, *129*, 11936–11949. (f) Hebden, T. J.; Penney, M. C.; Pons, V.; Piccoli, P. M. B.; Koetzle, T. F.; Schulz, A. J.; Kaminsky, W.; Goldberg, K. I.; Heinekey, D. M. *J. Am. Chem. Soc.* **2008**, *130*, 10812–10820. (g) Dietrich, B. L.; Goldberg, K. I.; Heinekey, D. M.; Autrey, T.; Linehan, J. C. *Inorg. Chem.* **2008**, *47*, 8583–8585. (h) Douglas, T. M.; Chaplin, A. B.; Weller, A. S. *J. Am. Chem. Soc.* **2008**, *130*, 14432–14433. (i) Rousseau, R.; Schenter, G. K.; Fulton, J. L.; Linehan, J. C.; Engelhard, M. H.; Autry, T. *J. Am. Chem. Soc.* **2009**, *131*, 10516–10524. (j) Douglas, T. M.; Chaplin, A. B.; Weller, A. S.; Yang, X.; Hall, M. B. *J. Am. Chem. Soc.* **2009**, *131*, 15440–15456. (k) Sloan, M. E.; Clark, T. J.; Manners, I. *Inorg. Chem.* **2009**, *48*, 2429–2435. (l) Zarmakiran, M.; Özkar, S. *Inorg. Chem.* **2009**, *48*, 8955–8964. (m) Dallanegra, R.; Chaplin, A. B.; Weller, A. S. *Angew. Chem., Int. Ed.* **2009**, *48*, 6875–6878. (n) Chaplin, A. B.; Weller, A. S. *Inorg. Chem.* **2010**, *49*, 1111–1121. (o) Chaplin, A. B.; Weller, A. S. *Angew. Chem., Int. Ed.* **2010**, *49*, 581–584.

(7) For other transition-metal-based catalysts, see, for example: (a) Clark, T. J.; Russell, C. A.; Manners, I. *J. Am. Chem. Soc.* **2006**, *128*, 9582–9583. (b) Keaton, R. J.; Blacquiere, J. M.; Baker, R. T. *J. Am. Chem. Soc.* **2007**, *129*, 1844–1845. (c) Pun, D.; Lobhovsky, E.; Chirik, P. J. *Chem. Commun.* **2007**, 3297–3299. (d) Jiang, Y.; Berke, H. *Chem. Commun.* **2007**, 3571–3573. (e) Pons, V.; Baker, R. T.; Szymczak, N. K.; Heldebrant, D. J.; Linehan, J. C.; Matus, M. H.; Grant, D. J.; Dixon, D. A. *Chem. Commun.* **2008**, 6597–6599. (f) Blaquiere, N.; Diallo-Garcia, S.; Gorelsky, S. I.; Black, D. A.; Fagnou, K. *J. Am. Chem. Soc.* **2008**, *130*, 14034–14035. (g) Jiang, Y.; Blacque, O.; Fox, T.; Frech, C. M.; Berke, H. *Organometallics* **2009**, *28*, 5493–5504. (h) Friedrich, A.; Drees, M.; Schneider, S. *Chem. Eur. J.* **2009**, *15*, 10339–10342. (i) Käss, M.; Friedrich, A.; Drees, M.; Schneider, S. *Angew. Chem., Int. Ed.* **2009**, *48*, 905–907. (j) Sloan, M. E.; Staubitz, A.; Clark, T. J.; Russell, C. A.; Lloyd-Jones, G. C.; Manners, I. *J. Am. Chem. Soc.* **2010**, *132*, 3831–3841.

(8) de los Ríos, I.; Tenorio, M. J.; Padilla, J.; Puerta, M. C.; Valerga, P. *Organometallics* **1996**, *15*, 4565–4574.

(9) Shaw, M. J.; Bryant, S. W.; Rath, N. *Eur. J. Inorg. Chem.* **2007**, 3943–3946.

(10) Synthesis of **6**: To solution of **4** (0.24 g, 0.16 mmol) in ca. 15 mL of C_6H_5F was added H_2BNCy_2 (0.59 mL of a 0.27 M solution in C_6H_5F, 0.16 mmol). After being stirred for 5 min, the solution was filtered and layered with hexanes (30 mL), and yellow crystals suitable for X-ray crystallography were obtained. Isolated yield, 0.08 g (32%). ^{1}H NMR (300 MHz, CD_2Cl_2, −20 °C): δ_H −14.56 (br, 1H, RuHB), 0.76−1.98 (overlapping m, 68 H, CH_2 and Cy of dcype, CH_2 of NCy), 2.90 (s, 1H, NCH), 3.30 (s, 1H, NCH), 4.77 (s, 5H, Cp), 5.80 (br, 1H, BH), 7.49 (s, 4H, *para*-CH of [BAr$^f_4$]$^-$), 7.65, (s, 8H, *ortho*-CH of [BAr$^f_4$]$^-$). ^{13}C{^{1}H} NMR (126 MHz, CD_2Cl_2, 20 °C): δ_C 22.0 (apparent t, $^1J_{PC}$ + $^2J_{PC}$ = 20 Hz, PCH_2 of dcype), 25.8−26.1 (br, CH_2 of NCy), 26.0, 26.4 (s, Cy C4 of dcype), 26.2, 28.9 (s, Cy C3 of dcype), 27.0, 27.1 (apparent t, $^2J_{PC}$ + $^4J_{PC}$ = 10 Hz, Cy C2 of dcype), 27.3, 27.4 (apparent t, $^2J_{PC}$ + $^4J_{PC}$ = 5 Hz, Cy C6 of dcype), 29.0, 29.2 (s, Cy C5 of dcype), 32.7, 38.1 (br, CH_2 of NCy), 38.2, 38.9 (apparent t, $^1J_{PC}$ + $^3J_{PC}$ = 14 Hz, PCH of dcype), 58.3, 64.2 (br, CH of NCy), 80.4 (s, Cp), 117.9 (*para*-CH of [BAr$^f_4$]$^-$), 125.0 (q, $^1J_{CF}$ = 272 Hz, CF_3 of [BAr$^f_4$]$^-$), 129.2 (q, $^2J_{CF}$ = 31 Hz, *meta*-C of [BAr$^f_4$]$^-$), 135.2 (*ortho*-CH of [BAr$^f_4$]$^-$), 162.0 (q, $^1J_{BC}$ = 50 Hz, *ipso*-C of [BAr$^f_4$]$^-$). ^{11}B{^{1}H} NMR (96 MHz, CD_2Cl_2, 20 °C): δ_B 35 (br, H_2BNCy_2), −7.6 ([BAr$^f_4$]$^-$). ^{19}F NMR (283 Hz, CD_2Cl_2, 20 °C): δ_F −62.7 (CF_3). ^{31}P{^{1}H} NMR (121 MHz, CD_2Cl_2, 20 °C): δ_P 81.4; (−80 °C) 79.2 (d, $^2J_{PP}$ = 23 Hz), 83.1 (d, $^2J_{PP}$ = 23 Hz). Microanalysis, calcd for $C_{75}H_{89}B_2F_{24}NP_2Ru$: C, 54.76; H, 5.45; N, 0.85. Found: C, 54.77; H, 5.47; N, 0.71.

(11) Euzenat, L.; Horhant, D.; Ribourdouille, Y.; Duriez, C.; Alcaraz, G.; Vaultier, M. *Chem. Commun.* **2003**, 2280–2281.

(12) Crystallographic data for **5**: $C_{85}H_{71}B_2F_{24}NP_2Ru$, M_r 1747.10, monoclinic, $P2_1/c$, a = 17.7779(1), b = 12.4782(1), and c = 35.9708(3) Å, β = 90.565(1)°, V = 7979.2(1) Å^3, Z = 4, ρ_c = 1.454 Mg m^{-3}, T = 150 K, λ = 0.71073 Å; 74 381 reflns collected, 18 022 independent

[R(int) = 0.049], which were used in all calculations; R_1 = 0.0566, wR_2 = 0.1169 for I > 2$\sigma(I)$, and R_1 = 0.1072, wR_2 = 0.1374 for all unique reflns; max and min residual electron densities 1.42 and −1.41 e Å^{-3}. CSD reference: 819704. Crystallographic data for **6**: $C_{75}H_{89}B_2F_{24}NP_2Ru$, M_r 1645.13, triclinic, $P\overline{1}$, a = 13.2296(2), b = 17.2074(3), and c = 17.6001(3) Å, α = 92.508(1), β = 103.503(1), and γ = 93.338(1)°, V = 3882.5(1) Å^3, Z = 2, ρ_c = 1.407 Mg m^{-3}, T = 150 K, λ = 0.71073 Å; 58 703 reflns collected, 17 192 independent [R(int) = 0.028], which were used in all calculations; R_1 = 0.0735, wR_2 = 0.1748 for I > 2$\sigma(I)$, and R_1 = 0.0969, wR_2 = 0.1930 for all unique reflns; max and min residual electron densities 2.20 and −1.63 e Å^{-3}. CSD reference: 819705.

(13) A ruthenium half-sandwich complex containing a κ^2-H_2BMes ligand has also been reported, featuring a Ru—B separation of 1.921(2) Å and a Ru···B—C angle of 172.3(2)°: Hesp, K. D.; Kannemann, F. O.; Rankin, M. A.; McDonald, R.; Ferguson, M. J.; Stradiotto, M. *Inorg. Chem.* **2011**, *50*, 2431–2444.

(14) For a related example of a κ^1-bound four-coordinate amine-borane, see: Kawano, Y.; Hashiva, M.; Shimoi, M. *Organometallics* **2006**, *25*, 4420–4426.

(15) For a recent review of σ borane complexes, see: Lin, Z. *Struct. Bonding (Berlin)* **2008**, *130*, 123–148.

(16) N.B.: The HOMO-2 orbital for the [CpML$_2$]$^+$ fragment lies perpendicular to the HOMO: Schilling, B. E. R.; Hoffmann, R.; Lichtenberger, D. *J. Am. Chem. Soc.* **1979**, *101*, 585–591.

(17) Schlecht, S.; Hartwig, J. F. *J. Am. Chem. Soc.* **2000**, *122*, 9435–9443.